



# Recrystallization of Cu-poor $\text{CuInS}_2$ assisted by metallic Cu or Ag

Humberto Rodriguez-Alvarez\*, Roland Mainz, Bjoern Marsen, Hans-Werner Schock

Helmholtz Zentrum Berlin für Materialien und Energie, Hahn-Meitner-Platz 1, 14109 Berlin, Germany

## ARTICLE INFO

### Article history:

Received 9 November 2009

Received in revised form

21 January 2010

Accepted 24 January 2010

Available online 1 February 2010

### Keywords:

Recrystallization

Thin-film solar cells

Energy-dispersive X-ray diffraction

## ABSTRACT

We monitor the recrystallization of Cu-poor  $\text{CuInS}_2$  thin films assisted by pure Cu or pure Ag by means of real-time synchrotron-based polychromatic X-ray diffraction. In both cases a new microstructure is formed accompanied by an increase in grain size. In the case of Cu, the onset temperature of the thin-film recrystallization is higher than 370 °C. In the case of Ag, the thin-film recrystallization comes to an end at 270 °C. The Ag-assisted recrystallization occurs in the presence of the body-centered cubic  $\beta\text{-Ag}_2\text{S}$  phase. We find that domain growth and diffusion of silver into the film occur simultaneously.

© 2010 Elsevier Inc. All rights reserved.

## 1. Introduction

Several fabrication techniques of  $\text{Cu}(\text{In,Ga})(\text{Se,S})_2$  thin films for solar cell absorbers make use of the recrystallization of small-grained (in the nanometer scale) Cu-poor material [1–4]. However, little is known about the solid state physics and chemistry of the recrystallization. In this work we report on the recrystallization of Cu-poor  $\text{CuInS}_2$  assisted by pure Cu or pure Ag. Ag is reported as an alloying element that increases the bandgap and decreases the structural disorder in  $(\text{Cu}_x\text{Ag}_{1-x})(\text{In}_y\text{Ga}_{1-y})\text{Se}_2$  thin films [5]. The same effects were looked for in  $(\text{Cu}_x\text{Ag}_{1-x})\text{InS}_2$  alloys without success [6]. In this paper we present experimental evidence that Ag lowers the recrystallization temperature of Cu-poor  $\text{CuInS}_2$  thin films.

## 2. Experimental

To isolate the recrystallization, layers of Cu-poor  $\text{CuInS}_2$  films were deposited on Mo-coated soda-lime glass substrates by means of physical thermal evaporation (PVD) in the following sequence: evaporation of indium at a substrate temperature of 275 °C and evaporation of Cu during a heating ramp to 580 °C in a sulfur atmosphere. Fig. 1(i) presents the cross-section of the films fabricated in this way. The films are Cu-poor with  $[\text{Cu}]/[\text{In}] \approx 0.9$  (measured by X-ray fluorescence analysis) and contain other than the  $\text{CuInS}_2$  phase approximately 10% in volume of the  $\text{CuIn}_5\text{S}_8$  spinel-type phase (estimated from an X-ray diffraction spectrum).

The layers present a small-grained morphology. A plane view taken in a scanning electron microscope (SEM) reveals grains in the form of plates (not shown here). From the plane view and cross-section SEM analyses we estimate the average grain size to be limited to few tens of nanometers. Pure Cu or Ag layers were deposited at room temperature on these Cu-poor  $\text{CuInS}_2$  layers so that the atomic ratio of group I atoms to group III atoms,  $[\text{I}]/[\text{III}]$ , was higher than 1. The thicknesses of the resulting bilayers (Cu-poor  $\text{CuInS}_2$  plus pure Cu or pure Ag) were measured in SEM cross-sections. The overall atomic ratios  $[\text{I}]/[\text{III}]$  of the bilayers were calculated using these thicknesses and the crystallographic densities. These were found to be approximately equal to: (a)  $[\text{Cu}]/[\text{In}] \approx 1.1$ , (b)  $[\text{Cu}]/[\text{In}] \approx 1.9$  and (c)  $[\text{Cu}+\text{Ag}]/[\text{In}] \approx 1.8$ , for the three bilayers fabricated. The relative error of these measurements is 15%.

The bilayers were then heated to 500 °C at a constant rate of  $1.44 \text{ K min}^{-1}$  in a vacuum chamber (base pressure is smaller than  $5 \times 10^{-4} \text{ mbar}$ ) that was coupled to the beamline for energy-dispersive X-ray diffraction (EDDI) of the Berlin synchrotron storage ring BESSY II [7]. The chamber had Al windows that are transparent for X-rays in the range between 10 and 100 keV. X-ray diffraction spectra were recorded as a function of the imposed temperature thanks to an energy-dispersive detector [8]. Energy-dispersive X-ray diffraction spectra (EDXRD) are characterized by the presence of Bragg reflections and fluorescence signals. The intensity of the  $\text{MoK}\alpha$  fluorescence line at 17.5 keV was used for normalization of the data to correct for overall intensity variations. The normalized intensities of the  $\text{InK}\alpha$  and  $\text{AgK}\alpha$  fluorescence lines at 24.2 and 22.2 keV were used to monitor qualitatively the distribution of In and Ag within the thin films. To complete the characterization the cross-sections of the heated films were analyzed in a SEM.

\* Corresponding author. Tel.: +49 30 8062 2737; fax: +49 30 8062 2931.

E-mail address: Humberto.rodriguez@helmholtz-berlin.de (H. Rodriguez-Alvarez).

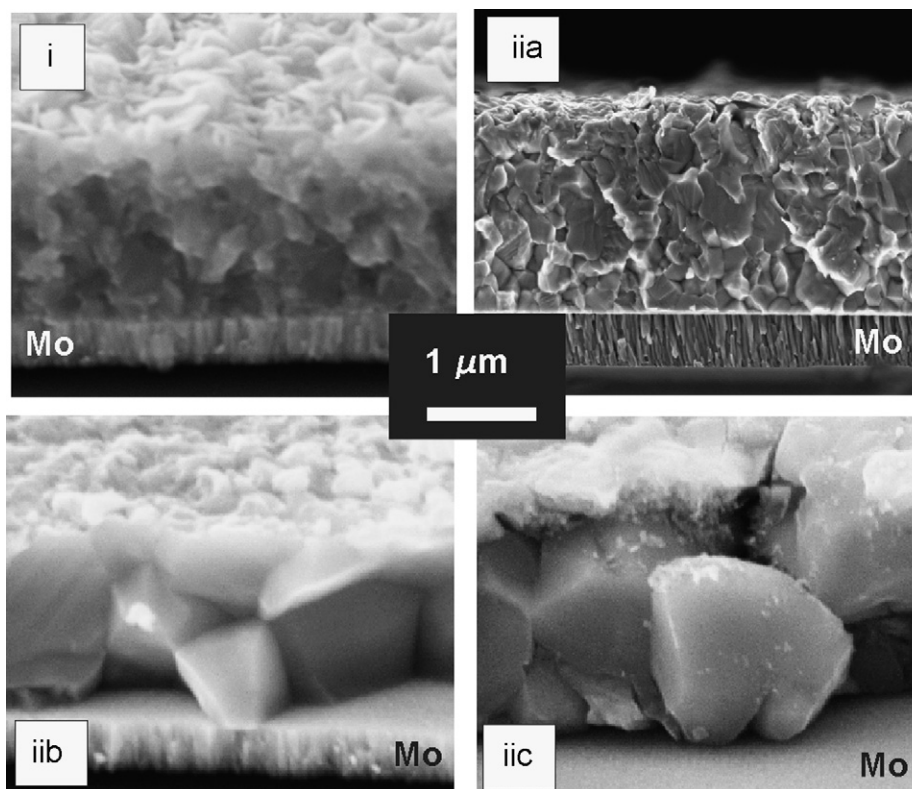


**Fig. 1.** SEM cross-sections: (i) Cu-poor  $\text{CuInS}_2$  ( $[\text{Cu}]/[\text{In}] \approx 0.9$ ) film (ii) after the deposition of a copper or silver layer and heating to  $500^\circ\text{C}$ . The overall atomic ratios before heating were  $[\text{Cu}]/[\text{In}] \approx 1.1$ ,  $[\text{Cu}]/[\text{In}] \approx 1.9$  and  $[\text{Cu}+\text{Ag}]/[\text{In}] \approx 1.8$  for (iia), (iib) and (iic) respectively. In (iib) the Cu-S phases were removed with KCN.

### 3. Results

Fig. 1(a–c) presents SEM cross-section images of the samples after the heating experiments. The images show that the average grain size increased compared to that of the initial Cu-poor layer shown in Fig. 1(i). In the case where the overall  $[\text{Cu}]/[\text{In}]$  ratio was approximately 1.1 (Fig. 1(iia)) the average grain size was found to be of the order of hundreds of nanometers whereas in the cases where the overall  $[\text{Cu}]/[\text{In}]$  ratio was approximately 1.9 (Fig. 1(iib)) and  $[\text{Cu}+\text{Ag}]/[\text{In}]$  approximately 1.8 (Fig. 1(iic)), the average grain sizes were of the order of some micrometers.

Fig. 2 presents the temperature-resolved EDXRD spectra in the energy range 28.8–31 keV recorded during the heating of the bilayers. The normalized intensity counts are color-coded. The Cu-poor  $\text{CuInS}_2$  112 reflections (Joint Committee of Powder Diffraction Standards file JCPDS 27-0159) were characterized by a large breadth at  $50^\circ\text{C}$ . During heating the breadth of this reflection was clearly reduced. A reduction of the breadth of an X-ray reflection is due to an increase in the domain size of coherent scattering [9]. The SEM cross-sections before and after the heating experiments (Fig. 1) coupled to the analysis of the corresponding 112  $\text{CuInS}_2$  reflections (Fig. 2) revealed that the decrease of the breadth is also accompanied by an increase in grain size. Therefore we interpret the decrease of the breadth of the 112 reflection as a measure of grain growth within the thin film.

In the case of  $[\text{Cu}]/[\text{In}] \approx 1.1$  the decrease of the breadth began shortly before  $400^\circ\text{C}$  and did not come to the detection end (where the breadth is determined by the instrumentation) at  $500^\circ\text{C}$ . In the case of  $[\text{Cu}]/[\text{In}] \approx 1.9$  the transition took place between  $410$  and  $440^\circ\text{C}$ . In the case of  $[\text{Cu}+\text{Ag}]/[\text{In}] \approx 1.8$  the transition was finished at  $270^\circ\text{C}$ . The white markers in the plots indicate the energetic position of the chalcopyrite 112 reflections that were extracted through a multiple line fit of the diffraction

data in the given energy range. The details on the fitting procedure are described in [10].

Fig. 3 presents the details on the heating of the bilayer with pure Ag. The evolution of the spectra was divided into five stages whose limits are marked by A, B, C and D in the figure. The different stages are described in the following points:

- The first Ag-S phase that was detected corresponded to the  $\alpha\text{-Ag}_2\text{S}$  monoclinic phase (JCPDS 14-0072) whose reflection signals grew steadily until  $T \approx 160^\circ\text{C}$  where the phase transition to the body-centered cubic  $\beta\text{-Ag}_2\text{S}$  [11] (JCPDS 04-0774) was observed (the expected transition temperature at normal pressure is  $T = 178^\circ\text{C}$  [12]). This phase is characterized by the 200 reflection at 39.3 keV in Fig. 3.
- Between (A) and (B) the intensities of the Ag 111 and 200 reflections and that of the  $\text{Ag}K\alpha$  fluorescence line decreased. In contrast to this, the intensity of the  $\text{In}K\alpha$  fluorescence line increased within this temperature range. Before (B) the  $\text{CuIn}_5\text{S}_8$  400 reflection (JCPDS 24-0361) shifted to lower energies (larger lattice constants). We interpret this as the appearance of the solid solution  $\text{Cu}_{1-x}\text{Ag}_x\text{In}_5\text{S}_8$  reported in [13] and its consequent enrichment in Ag. At (B) this reflection vanished indicating the consumption of the spinel-type phases. From this temperature on, the reflection at 29.5 keV was unambiguously attributed to the  $\text{Cu}_{1-x}\text{Ag}_x\text{InS}_2$  phase.
- Between (B) and (C) the  $\text{Cu}_{1-x}\text{Ag}_x\text{InS}_2$  112 reflection shifted to higher energies (smaller lattice constants), its intensity increased and its breadth decreased. The decrease of the breadth occurred simultaneously to the further cross-over of the normalized  $\text{Ag}K\alpha$  and  $\text{In}K\alpha$  intensities. Both processes ended at the same temperature where the intensity of the  $\text{CuInS}_2$  112 reflection vanishes. At this temperature the 103

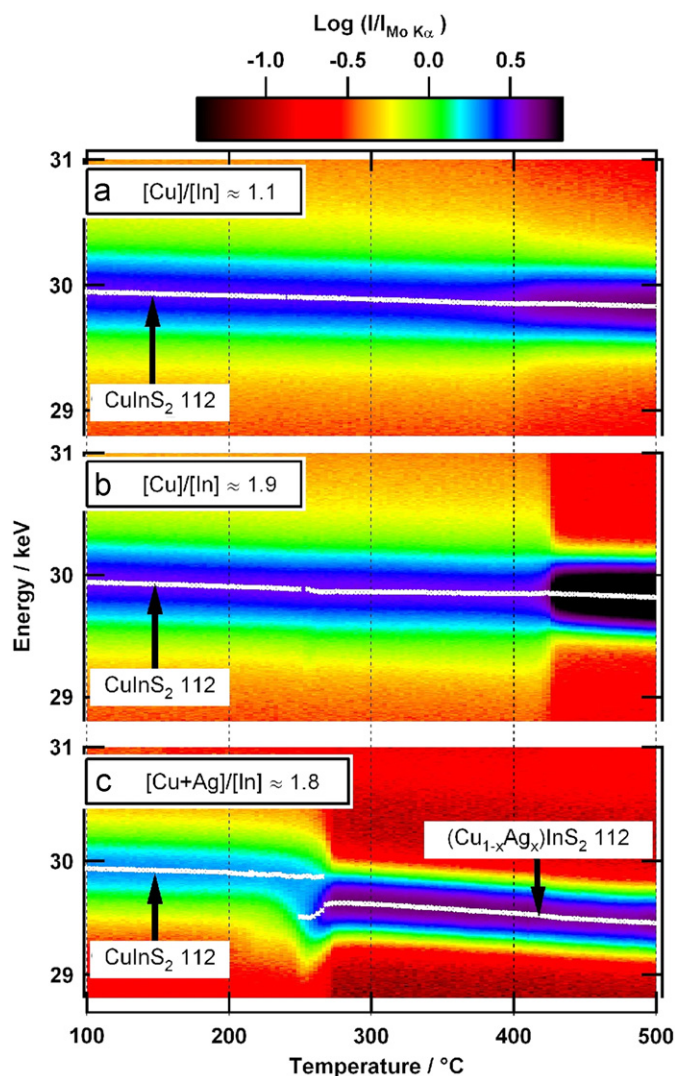


**Fig. 2.** Temperature-dependent energy-dispersive X-ray diffraction spectra recorded during heating of the three bilayers. This energy range, 28.8–31 keV, includes the 112 reflection of the  $\text{CuInS}_2$  and  $\text{Cu}_{1-x}\text{Ag}_x\text{InS}_2$  phases.

and 105/213 chalcopyrite reflections emerge at 30.8 and 46.0 keV. These reflections stem from the cation ordering in the chalcopyrite structure.

- At (D) the face-centered cubic  $\text{Ag}_{1.2}\text{Cu}_{0.8}\text{S}$  phase (JCPDS 12-0154) appeared. During cool down (not shown here) the reflections attributed to this phase vanished and the reverse phase transition  $\beta\text{-Ag}_2\text{S}$  to  $\alpha\text{-Ag}_2\text{S}$  was observed.

#### 4. Discussion

We divide the recrystallization of Cu-poor nanocrystalline  $\text{CuInS}_2$  material in three steps: the consumption of the  $\text{CuIn}_5\text{S}_8$  spinel-type phase, the increase in grain size and the ordering of the cations in the chalcopyrite structure. The degree of recrystallization depends on the nature of the group I elements and on the [I]/[III] ratio. Increasing the [I]/[III] ratio reduces the temperature range in which the grain growth takes place. However, the onset of the grain growth remains above 370 °C when using metallic Cu (with  $1.1 < [\text{I}]/[\text{III}] < 1.9$ ). In contrast to this, alloying with metallic Ag reduces the onset temperature to

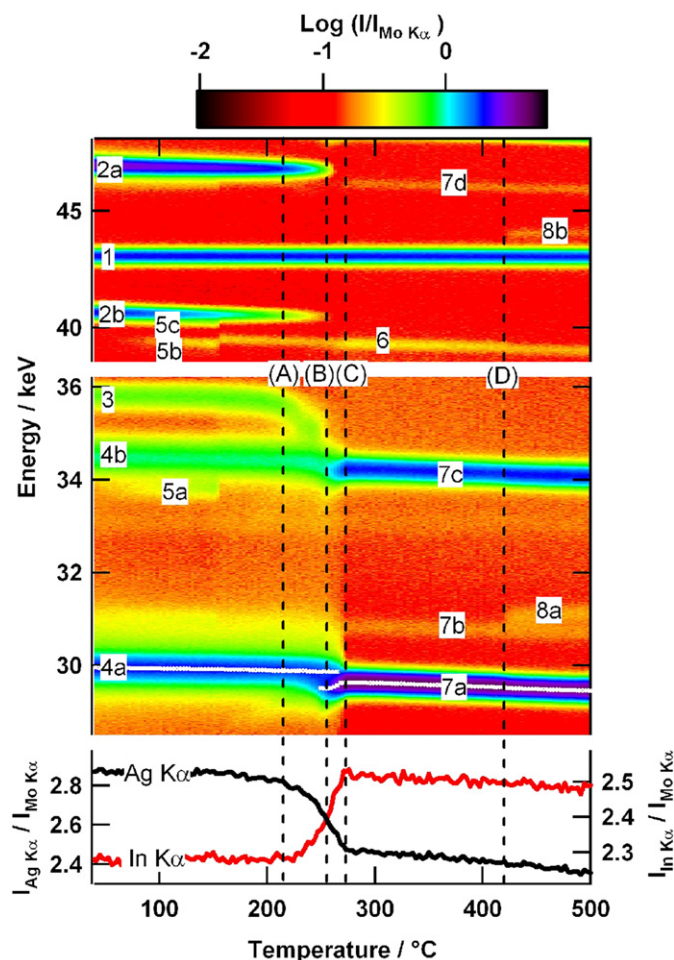


**Fig. 3.** Temperature-dependent energy-dispersive X-ray diffraction spectra and normalized integral intensities of the  $\text{AgK}\alpha$  and  $\text{InK}\alpha$  fluorescence lines recorded during heating of the Cu-poor  $\text{CuInS}_2/\text{Ag}$  bilayer. The X-ray reflections correspond to: (1) Mo 110; (2a and b) Ag 200 and 111; (3)  $\text{CuIn}_5\text{S}_8$  400; (4a and b)  $\text{CuInS}_2$  112 and 200/004; (5a–c)  $\alpha\text{-Ag}_2\text{S}$  112, 121 and -103; (6)  $\beta\text{-Ag}_2\text{S}$  200; (7a–d)  $\text{Cu}_{1-x}\text{Ag}_x\text{InS}_2$  112, 103, 200/004, 105/213; (8a and b)  $\text{Ag}_{1.2}\text{Cu}_{0.8}\text{S}$  200 and 220.

$\approx 250$  °C. The recrystallization comes to an end at 270 °C when using metallic Ag (with  $[\text{I}]/[\text{III}] \approx 1.8$ ).

We monitored the diffusion of Ag into the Ag-free  $\text{CuInS}_2$  film by analyzing the intensity of the normalized  $\text{AgK}\alpha$  and  $\text{InK}\alpha$  fluorescence signals. The intensity of the  $\text{AgK}\alpha$  fluorescence line decreases as Ag diffuses into the Cu-poor  $\text{CuInS}_2$  film because it is increasingly absorbed by Cu and In. The intensity of the  $\text{InK}\alpha$  fluorescence line increases as Ag diffuses into the  $\text{CuInS}_2$  film because the absorption due to Ag decreases. We observed two main points in the Ag-triggered recrystallization: (1) the increase in grain size characterized by the decrease of the breadth of the  $\text{Cu}_{1-x}\text{Ag}_x\text{InS}_2$  112 reflection is coupled to the diffusion of Ag into the film characterized by the cross-over of the  $\text{AgK}\alpha$  and  $\text{InK}\alpha$  fluorescence intensities; (2) the increase in grain size occurs in presence of the  $\beta\text{-Ag}_2\text{S}$  phase. The second point questions some of the grain growth models of chalcopyrite thin films that are based on the hypothesis that a face-centered cubic secondary phase is necessary for cationic transport. These models are based on the fact that in the chalcopyrite and sphalerite structure, the anions are also present in a face-centered cubic sublattice [14,15]. In the case of the Ag-triggered recrystallization, grain growth occurs in the presence of the  $\beta\text{-Ag}_2\text{S}$  phase where the anions are placed in a body-centered cubic arrangement [16]. We suggest that the cation mobility within the chalcopyrite phase controls grain

growth. Increasing the cation mobility should enhance the recrystallization. Ag cations are more mobile than Cu cations in  $\text{Cu}_{1-x}\text{Ag}_x\text{InSe}_2$  [17]. Knowing this and the melting points of  $\text{AgInS}_2$  and  $\text{CuInS}_2$  (871 and 1079 °C respectively), we suppose that Ag cations are also more mobile than Cu cations in  $\text{Cu}_{1-x}\text{Ag}_x\text{InS}_2$ .

## 5. Conclusions

In conclusion, we monitored *in-situ* for the first time the recrystallization of Cu-poor  $\text{CuInS}_2$  thin films assisted by pure metallic Cu or Ag. The recrystallization includes the consumption of the spinel-type phases, the growth of grains and the ordering of the cations in the chalcopyrite phase. When using pure metallic Cu, the  $[\text{Cu}]/[\text{In}]$  ratio determines the temperature range and the onset of the grain growth. Using Ag lowers the recrystallization temperature to 270 °C. In this case, grain growth is coupled to the diffusion of Ag into the film. Grain growth occurs in the presence of the body-centered cubic  $\beta\text{-Ag}_2\text{S}$  phase. We conclude that: i) the diffusion of the cations and their mobility within the chalcopyrite phase play a primary role in the recrystallization, and ii) face-centered cubic secondary Cu-S phases are not a necessary condition to obtain large-grained  $\text{CuInS}_2$  materials.

## References

- [1] J. Schoeldstroem, J. Kessler, M. Edoff, *Thin Solid Films* 480 (2005) 61–66.
- [2] O. Volobujeva, J. Kois, R. Traksmaa, K. Muska, S. Bereznev, M. Grossberg, E. Mellikov, *Thin Solid Films* 516 (2008) 7105–7109.
- [3] M. Krunk, *Appl. Surf. Sci.* 142 (1999) 356–361.
- [4] Q. Guo, S.J. Kim, M. Kar, W.N. Shafarman, R.W. Birkmire, E.A. Stach, R. Agrawal, H.W. Hillhouse, *Nano Lett.* 8 (9) (2008) 2982–2987.
- [5] P.T. Erslev, G.M. Hanket, W.N. Shafarman, J.D. Cohen, in: *Proceedings of the Materials Research Society, Spring Meeting 2009, Symposium M, 2009, 1165-M01-07*.
- [6] A. Werner, I. Luck, J. Bruns, J. Klaer, K. Siemer, D. Braeunig, *Thin Solid Films* 361–362 (2000) 88–93.
- [7] C. Genzel, I.A. Denks, J. Gibmeier, M. Klaus, G. Wagener, *Nucl. Instrum. Meth.: Phys. Res. A* 578 (1) (2007) 23–33.
- [8] H. Rodriguez-Alvarez, I.M. Koetschau, H.W. Schock, *J. Cryst. Growth* 310 (15) (2008) 3638–3644.
- [9] T. Ungar, *Scr. Materialia* 51 (2004) 777–781.
- [10] H. Rodriguez-Alvarez, R. Mainz, A. Weber, B. Marsen, H.-W. Schock, in: *Proceedings of the Materials Research Society, Spring Meeting 2009, Symposium M, 2009, 1165-M02-07*.
- [11] S. Djurle, *Acta Chemica Scand.* 12 (1958) 1427–1436.
- [12] R.C. Sharma, Y.A. Chang, *Bull. Alloy Phase Diagr.* 7 (3) (1986) 263.
- [13] I.V. Bodnar, E.A. Kudritskaya, I.K. Polushina, V.Y. Rud, Y.V. Rud, *Semiconductors* 32 (9) (1998) 933–936.
- [14] T. Wada, N. Kohara, T. Negami, M. Nishitani, *J. Mat. Res.* 12 (6) (1997) 1456.
- [15] D. Abou-Ras, R. Caballero, C. Kaufmann, M. Nichterwitz, K. Sakurai, S. Schorr, T. Unold, H.W. Schock, *Phys. Stat. Sol. (RRL)* 2 (3) (2008) 135–137.
- [16] K. Bozhilov, V. Dimov, A. Panov, H. Haefke, *Thin Solid Films* 190 (1) (1990) 129–138.
- [17] G. Dagan, T.F. Ciszek, D. Cahen, *J. Phys. Chem.* 96 (26) (1992) 11009–11017.